Available online at www.sciencedirect.com
SCIENCE DIRECT
Journal of Photochemistry and Photobiology A: Chemistry 177 (2006) 238–247
Journal of Photochemistry and Photobiology A:Chemistry
www.elsevier.com/locate/jphotochem

Photophysics of benzazole derived push–pull butadienes: A highly sensitive fluorescence probes

Safaa El-Din H. Etaiw, Tarek A. Fayed*, Naglaa Z. Saleh

Chemistry Department, Faculty of Science, Tanta University, Al-Geish Street, Tanta 31527, Egypt

Received 26 March 2005; received in revised form 24 May 2005; accepted 31 May 2005
Available online 5 July 2005

Abstract

Two new homologues of 1,4-diphenylbutadiene, namely, 1-(2-benzazolyl)-4-(*p*-dimethylaminophenyl)buta-1,3-diene have been synthesized and their absorption and fluorescence properties have been investigated in different organic solvents. The absorption spectra are less sensitive to the solvent polarity than the corresponding fluorescence spectra, which show dual emission and high solvatochromic effect in polar solvents. Using an efficient solvatochromic method, a large excited state dipole moment parallel to the smaller ground state dipole moment was calculated. Other properties of the lowest excited state such as the planar ICT B_u nature, fluorescence quantum yield and the basicity of the two nitrogen atoms (of the benzoxazole or benzothiazole ring as well as the amino group) were studied by spectroscopic techniques and semiempirical AM1 quantum chemical calculations. The findings have been presented and discussed along with the promising fluorescence probing and pH-sensing properties of these two dienes. The main spectroscopic properties of the two derivatives have been also compared.

Keywords: Diphenylbutadiene; Fluorescence probing; ICT; Benzoxazole; Benzothiazole; Semiempirical; Dipole moment; Viscosity

1. Introduction

Linear polyenes have attracted a great deal of attention as models of the retinyl polyenes that are related to Vitamin A and the opsin family of proteins responsible for biological sensory (such as vision) and photoenergy transduction [1,2]. All-*trans*-diphenylpolyenes belong to the C_{2h} point group and their ground states are characterized by A_g symmetry while the excited singlet π–π^* state can have either A_g or B_u symmetry [3,4]. The excited state properties of these polyenes are governed by several factors including the order of symmetry of the two lowest-lying excited states, their electronic energy gap, interstate mixing and the dynamics of photoisomerization. The A_g state is covalent in nature and hence is insensitive to the solvent polarity. In contrast, the B_u state is ionic, so it is stabilized in polar solvents. For 1,4-diphenylbutadiene, the energy gap between the two lowest excited states ($2A_g$ and $1B_u$) is rather small [5]. Therefore, small changes in molecular structure or solvent orientation can affect the relative lowering of these states.

The photophysical and photochemical properties of 1,4-diphenylpolyenes have been the subject of many investigations [6,7]. Particular attention has been given to the donor–acceptor-diphenylbutadienes in connection with their non-linear optical properties, e.g. large hyperpolarizabilities as well as the long-distance intramolecular charge transfer (ICT) [8–11]. The excited state properties of several donor–acceptor-substituted diphenylbutadienes have been examined in homogeneous [3,12–16] and microheterogeneous media [17–20]. It has been argued that there is one more excited state of twisted nature (more polar and less energetic) other than the locally and perpendicular excited states, which controls the photoprocesses of such compounds. However, the exact nature of the excited state of these polyenes and the mechanism of functions of linear polyene-based photoreceptors are not clearly known. Therefore, synthesis of new polyenes and characterization of their photophysical properties in different environments, are necessary prereq-

* Corresponding author. Tel.: +20 40 3120708; fax: +20 40 3350804.
E-mail addresses: safaaehe@gega.net (S.E.-D.H. Etaiw), tfayed2003@yahoo.co.uk (T.A. Fayed).

1010-6030/$ – see front matter © 2005 Elsevier B.V. All rights reserved.
doi:10.1016/j.jphotochem.2005.05.029

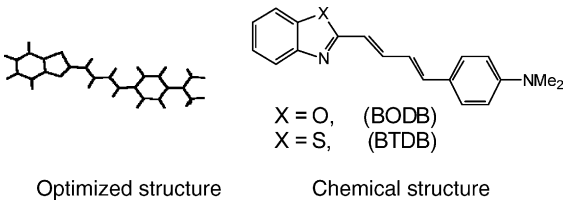

Scheme 1.

uisites for further research in modern technologies. So, 1,4-diphenylpolyenes in which one or the two phenyl rings are replaced by heterocyclic rings (such as pyridine [21–26] or thiophene [26,27]) or polycyclic aromatic groups (such as anthryl [26,28], pyrenyl [26,29] or quinazolin-4-only [30]) have been synthesized and their spectral as well as photochemical properties have been investigated. These butadiene derivatives display important differences in their photophysical properties since the aromatic groups strongly affect the nature of the lowest excited singlet state and the shape of the potential energy surface for *trans*/*cis* photoisomerization [26].

Recently, we have studied the photophysics and photochemistry of benzothiazole and benzoxazole homologues of 4-dimethylaminostilbene [31–34]. These molecules act as push–pull ethylenes, which can be utilized as good reporters for their microenvironment [31–33]. In continuation of our work with donor–acceptor fluorescent molecules based on benzazoles, we have synthesized two new homologues of 1,4-diphenylbutadiene, namely, 1-(2-benzoxazolyl)-4-(*p*-dimethylamino- phenyl)buta-1,3-diene, BODB, and its 2-benzothiazolyl derivative, BTDB. The molecular structure of these two dienes is displayed in Scheme 1. Each molecule differs from the styrylbenzazole by a single C=C unit. Extension of the chain length is associated with changes in electron delocalization within the molecule. To account for these properties we have studied the steady state absorption and emission properties of two new fluorescence probes, based on the ICT mechanism, in different organic solvents. This is to gain information about the nature of the electronic excited states responsible for the dual emission in polar solvents. Also, the ground and excited state dipole moments have been calculated from the solvatochromic shifts and compared with the values obtained from semi-empirical calculations. Benzoxazole and benzothiazole derivatives have widespread applications based on their clinical efficacy as an anti-tumor [35] and anti-HIV activity [36]. They are also suitable sensitizers for photographic halide emulsions [37] and have high non-linear optical effectiveness [38].

2. Experimental

2.1. Materials

Starting materials and reagents for the synthesis of dienes BODB and BTDB were obtained from Fluka and used without further purification. For spectroscopic studies, UV-grade organic solvents (all Aldrich) were used after drying.

2.1.1. Synthesis of 1-(2-benzazolyl)-4-(*p*-dimethylaminophenyl)buta-1,3-dienes

In typical procedures, 0.01 mol 2-methylbenzoxazole (or 2-methylbenzothiazole) was dissolved in 50 ml DMF containing 2.5 g NaOH, and were taken in a two-necked flat bottom flask. The mixture was magnetically stirred at ambient temperature for 10 min after which a solution of *p*-(dimethylamino)cinnamaldehyde, 0.01 mol in 10 ml DMF, was added. The stirring was continued under dark conditions until most of the aldehyde had reacted (ca. 3 h) as indicated by thin layer chromatographic analysis. After completion of the reaction, the reaction mixture was quenched with acidified water (pH was reduced to 6–7 by adding conc. HCl). The crude product was filtered off and purified by recrystallization twice from ethanol. The separated orange-red crystals were characterized by elemental analysis and ^{1}H NMR.

2.2. Methods and instrumentation

Aqueous buffer solutions were prepared by mixing appropriate volumes of NaOH and H_3PO_4 (0.1 M each). Solutions having pH < 2 were prepared following Hammett's acidity (H_o) scale [39].

The UV–vis-absorption spectra were measured by using a Shimadzu UV-3101PC scanning spectrophotometer. The fluorescence measurements were done on a Perkin-Elmer LS 50B spectrofluorimeter fitted with a temperature controlled unit (Fischer Scientific Isotherm Refrigerated Circular Model 9000). The fluorescence quantum yield (ϕ_f) was measured relative to quinine sulphate (ϕ_f = 0.54 in 0.1 M H_2SO_4) [40]. In all measurements, freshly prepared 2×10^{-5} M solutions were used and handled under dim light.

2.3. Theoretical calculations

Semiempirical molecular orbital calculations were carried out for BODB and BTDB at the AM1 level using the HyperChem software (Version 5.11) [41]. Fully optimized ground state geometry is shown in Scheme 1 while the calculated net charges on some selected atoms, heat of formation and the ground state dipole moment of both dienes are given in Table 3.

3. Results and discussion

3.1. Solvent-induced shifts of absorption and emission spectra

The absorption and fluorescence spectra of the investigated butadienyl benzazoles (BODB and BTDB) were recorded in several solvents of different polarity and proton donating ability at room temperature. Fig. 1 shows the absorp-

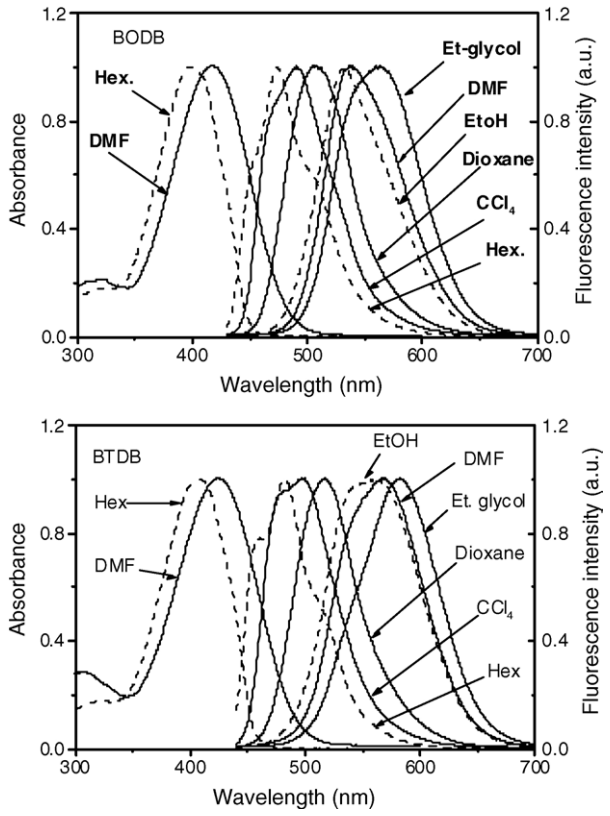

Fig. 1. Normalized absorption and fluorescence spectra of BODB (upper panel) and BTDB (lower panel) in solvents of different polarity.

tion spectra in *n*-hexane and DMF as examples of non-polar and polar solvents, respectively, as well as representative fluorescence spectra, while the corresponding spectral data are summarized in Table 1.

The absorption spectra of BODB and BTDB display an intense broad band in the range 350–500 nm. The molar extinction coefficients at the wavelength of maximum absorption (ε_{max}) are high. Their values are in the range $(37–43) \times 10^3\ M^{-1}\ cm^{-1}$ and $(74–85) \times 10^3\ M^{-1}\ cm^{-1}$ for BTDB and BODB, respectively. The absorption maximum is significantly red-shifted (ca. 18 nm) as the solvent polarity is increased from *n*-hexane to DMF. The effect of solvent polarity on the absorption maximum is shown by plot of the absorption energy $E(A)$ as a function of the corresponding values of the Reichardt's dye, $E_T(30)$ scale [42] (Fig. 2). This scale is an empirical measure of the proton-donating ability and the polarizability of solvents. However, the correlations are fair ($r = 0.79–0.80$) but indicate a low sensitivity to the solvent polarity as reflected from their slopes (0.09 and 0.045 in the case of BODB and BTDB, respectively). The red-shifted absorption spectra in polar solvents as well as the high molar absorptivity point to an allowed B_u character of the electronic state reached by light absorption, which is preferentially stabilized by solvents of high polarity.

Conversely, the fluorescence maximum is greatly affected by the solvent polarity where a much red-shifted fluorescence is observed on increasing the solvent polarity (Fig. 1). Such a behaviour indicate that the fluorescent state is not the same as the initially populated excited state (locally excited state, LE), but it is a highly polar state with a charge transfer characters (ICT state). The solvent-induced shift of the fluorescence maximum is also represented by the plot of the fluorescence energy $E(F)$ versus $E_T(30)$ as shown in Fig. 2, where a double linear correlation is found for both dienes. Alcoholic solvents fall on a separate line (having a higher slope) indicating that the mode of solvation of the emitting state is different from that in the other polar aprotic solvents. Probably due to hydrogen bonding interactions. In fact, the correlations are

Table 1
Absorption and fluorescence characteristics of BODB and BTDB measured in pure solvents at 25 °C

Solvent	BODB				BTDB			
	λ_{max} (nm)		$\Delta\nu_{st}$ (cm^{-1})	ϕ_f	λ_{max} (nm)		$\Delta\nu_{st}$ (cm^{-1})	ϕ_f
	abs	em			abs	em		
n-Hexane	401	474	3841	0.0176	405	478	3786	0.022
CCl_4	406	491	4310	–	415	499	4090	–
Toluene	413	496	4070	0.0078	419	500	3852	0.0088
Benzene	411	503	4447	–	420	504	3961	–
Dioxane	411	508	4654	–	416	516	4701	–
$CHCl_3$	414	517	4838	–	420	526	4809	–
CH_2Cl_2	415	525	5080	0.0048	421	533	5005	0.0054
Acetone	409	531	5619	–	419	557	5919	–
DMF	419	538	5292	0.007	423	567	6035	0.0064
CH_3CN	410	535	5742	0.0055	415	562	6081	0.0068
BuOH	417	525	4936	0.0045	424	531	4753	0.0044
PrOH	417	526	5003	0.0045	423	533	4865	0.0054
EtOH	417	531	5156	0.0048	422	560	5844	0.0045
MeOH	417	539	5445	0.0045	422	573	6269	0.0039
Et-glycol	424	562	5782	0.0088	431	583	6044	0.0062
Glycerol	424	566	5901	0.0359	432	583	6005	0.039

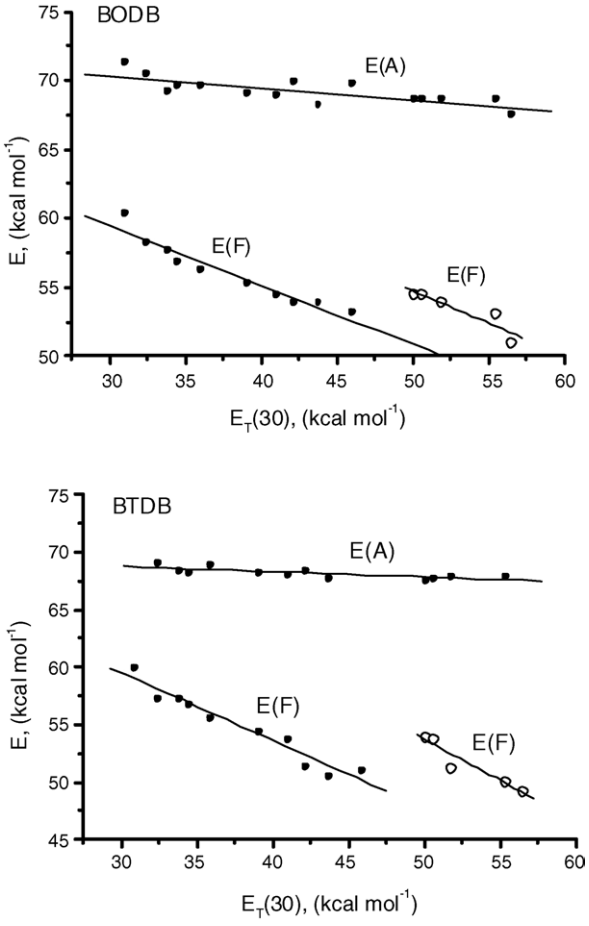

Fig. 2. Dependence of the absorption [$E(A)$] and fluorescence [$E(F)$] energies of BODB and BTDB on the empirical solvent polarity parameter, $E_T(30)$.

much stronger ($r = 0.92$–0.97) and their slopes (in the range 0.43–0.72) reflect the high sensitivity of $E(F)$ to the solvent polarity. The enhanced solvent sensitivity of $E(F)$ compared to $E(A)$ can be attributed to increased solute–solvent interactions in the excited state due to an increased dipole moment upon excitation.

Another feature that can be easily observed from Fig. 1 is that the fluorescence spectra seem to result from more than one component where a hint of structure can be observed in polar solvents. In order to quantify these changes, representative spectra have been fitted as a sum of two Gaussian peaks with the help of a Gaussian curve-fitting programme. Fig. 3 displays the deconvoluted spectra of BODB and BTDB in some polar solvents. The area under the peak and the height of each peak with the corresponding λ_{max} are given in Table 2. One possibility for explaining the appearance of the large red shifted fluorescence is the participation of a polar ICT state and/or formation of hydrogen-bonded complexes in polar protic solvents. However, attribution of this band to fluorescence from a hydrogen-bonded complex can be ruled out based on the fact that the long-wavelength fluorescence band is also observed in aprotic solvents, e.g. DMF.

Table 2
Area under the curve, emission maximum and height of the peak obtained from Gaussian curve fitting analysis of the fluorescence spectra

Solvent	Peak	BODB			BTDB		
		λ_{max}	Area	Height	λ_{max}	Area	Height
EtOH	ICT	555	54.9	0.63	566	89.9	0.97
	LE	526	22.9	0.49	530	8.2	0.23
DMF	ICT	562	59.4	0.72	569	84.4	0.98
	LE	530	21.2	0.49	535	5.6	0.17
Et-glycol	ICT	569	77.8	0.95	584	79.1	0.93
	LE	535	10.4	0.27	545	7.9	0.11

As can be seen from Fig. 3, the intensity of the ICT emission increases as the polarity and viscosity of the medium is increased while that of the LE emission shows an opposite dependence.

In addition, the spectral data in Table 1 shows that the Franck–Condon absorption and fluorescence transitions of BTDB are bathochromically shifted in comparison to those of BODB in all solvents. However, the pronounced red shift of the absorption maximum is small (≈4–6 nm). In contrast, the corresponding shift of the fluorescence maximum is large (≈4–30 nm), depending on the solvent polarity. These results indicate that the charge transfer interaction of the $-NMe_2$ group is larger with the benzothiazole (BT) moiety than with the benzoxazole (BO) one. This is confirmed by the finding that the intensity of the ICT emission of BTDB is higher relative to that of BODB when compared in the same solvent (see Fig. 3). Based on the charge density calculations, Table 3, it appears that the electronegativity of the benzazole ring is in the order BT > BO. This can be easily observed from the higher positive charge calculated for the S-atom and the considerable negative charge calculated for the O-atom. This observation is in agreement with that reported previously for 2-(*p*-dimethylaminophenyl)benzazoles [43].

Moreover, the data in Table 1 indicates that the fluorescence quantum yield, ϕ_f, of BODB and BTDB decreases as the solvent polarity increases from *n*-hexane to CH_3CN. The lower ϕ_f-values in polar solvents can be attributed to enhanced ICT interaction, which often results in fluorescence quenching. Also, the ϕ_f-value is much higher in ethylene glycol and glycerol. This is due to increasing of frictional forces and decreasing of free volume necessary for rotation dependent radiationless *trans–cis* photoconversion around the double bonds. In alcohols, the ϕ_f-values are lower than those in aprotic solvents having higher dielectric constants such as DMF and CH_3CN. Such behaviour can be attributed to hydrogen bonding effect, which enhances the non-radiative internal conversion.

3.2. Dipole moment calculations

The ICT excited state can also be investigated through estimation of the difference in the dipole moments between

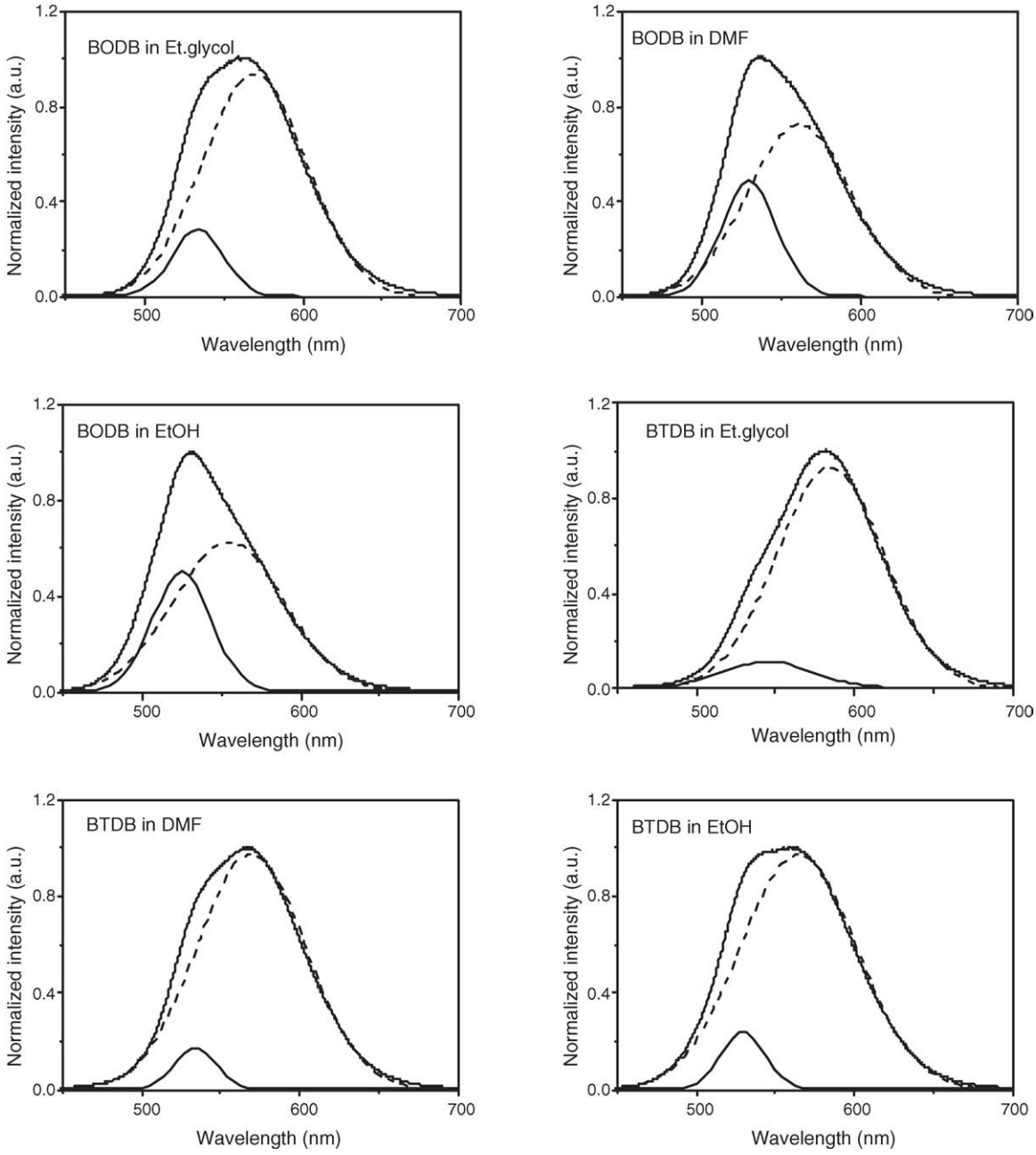

Fig. 3. Deconvoluted fluorescence spectra of BODB and BTDB in the mentioned polar solvents.

the excited singlet (μ_e) and ground (μ_g) states. This can be achieved by analysis of the solvatochromic spectral shifts using Lippert equations [44]:

$$\bar{\nu}_A - \bar{\nu}_F = m_1 f(\varepsilon, n) + \text{constant} \quad (1)$$

$$\bar{\nu}_A + \bar{\nu}_F = m_1[f(\varepsilon, n) + 2g(n)] + \text{constant} \quad (2)$$

where $\bar{\nu}_A$ and $\bar{\nu}_F$ are the absorption and emission band maxima in cm^{-1}, measured in solvent of different permitivities

Table 3
Heat of formation (ΔH_f, kcal/mol) and the net charges on selected molecular subunits, calculated after geometrical optimization of the ground state

Diene	ΔH_f	Net charge on					
		Dimethyl aniline	Butadiene bridge	Benzazole moiety	*N*-amino	*N*-hetero	X (O or S)
BODB	92.31	0.0213	0.1227	−0.1439	−0.2637	−0.1364	−0.1339
BTDB	114.05	0.0138	0.0894	−0.1033	−0.2597	−0.1041	0.3992

(ε) and different refractive indices (n):

$$m_1\frac{2(\mu_e-\mu_g)^2}{hca^3}=\frac{2(\mu_e^2+\mu_g^2-2\mu_e\mu_g\cos\psi)}{hca^3}\quad\text{and}$$

$$m_2=\frac{2(\mu_e^2-\mu_g^2)}{hca^3} \tag{3}$$

where h is the Planck's constant, c the speed of light in vacuum and a is the Onsager's interaction radius of the solute. According to this model, the polarizability term ($2\alpha/a^3$) including the solute polarizability (α) was neglected and the solvent polarity functions are given by

$$f(\varepsilon,n)=\frac{\varepsilon-1}{2\varepsilon+1}-\frac{n^2-1}{2n^2+1}\quad\text{and}\quad g(n)=\frac{n^2-1}{2n^2+1} \tag{4}$$

If the ground and excited state dipole moments are parallel, based on Eq. (3), the following equations can be derived [45]:

$$\mu_g=\frac{m_2-m_1}{2}\left(\frac{hca^3}{2m_1}\right)^{1/2}\quad\text{and}$$

$$\mu_e=\frac{m_2+m_1}{2}\left(\frac{hca^3}{2m_1}\right)^{1/2} \tag{5}$$

$$\mu_e=\frac{m_2+m_1}{m_2-m_1}\mu_g\quad\text{for}\,m_2>m_1 \tag{6}$$

The following correlations were obtained from the spectral shifts with solvent polarity, for BODB:

$$\bar{\nu}_A-\bar{\nu}_F=3997+5348\,f(\varepsilon,n)\quad(r=0.98) \tag{7}$$

$$\bar{\nu}_A+\bar{\nu}_F=48729-8904[f(\varepsilon,n)+2g(n)]\quad(r=0.95) \tag{8}$$

whereas for BTDB:

$$\bar{\nu}_A-\bar{\nu}_F=3753+7577\,f(\varepsilon,n)\quad(r=0.97) \tag{9}$$

$$\bar{\nu}_A+\bar{\nu}_F=49051-11081[f(\varepsilon,n)+2g(n)]\quad(r=0.96) \tag{10}$$

Alcohols were excluded from these correlations to avoid specific solute–solvent interactions.

The Onsager's model assumes that the cavity radius containing the probe is spherical. However, the molecules under study show an ellipsoidal shape. Thus, μ_e has been calculated without any assumption about the cavity radius using Eq. (6) and the μ_g-value obtained from semiempirical AM1 calculations. The excited and ground state dipole moments were also determined using Eq. (5) and the calculated Onsager's cavity radius. The Onsager's cavity radius was taken as 40% from the long axis of the molecule [46] which was calculated after geometry optimization, for BODB and BTDB are a = 6.4 and 6.8 Å, respectively. The dipole moment values are collected in Table 4 together with the slopes of the corresponding solvatochromic shifts. A glance at these data reveals a good agreement between the values obtained from the ratio method (Eq. (6)) and those obtained using the calculated radius (Eq. (5)).

Furthermore, the angle (ψ) between orientation of the ground and excited state dipole moments was calculated using Eq. (11) [45] which can be obtained directly from Eq. (3):

$$\cos\psi=\frac{1}{2\mu_e\mu_g}\left[(\mu_g^2+\mu_e^2)-\frac{m_1}{m_2}(\mu_g^2-\mu_e^2)\right] \tag{11}$$

For the compounds under study, ψ-value is close to 0 ($\cos\psi\approx1.0$), thus, it could be concluded that the vectors of the ground and excited state dipole moments are parallel.

Also, the dipole moment of the Franck–Condon excited state (μ^{FC}) was calculated from the solvatochromic shift of the absorption spectra using Eq. (12) [20]:

$$\bar{\nu}_A=\bar{\nu}_A^o-\frac{2\mu_g(\mu^{FC}-\mu_g)}{hca^3}[f(\varepsilon,n)] \tag{12}$$

where

$$f(\varepsilon,n)=\frac{\varepsilon-1}{2\varepsilon+1}-0.5\frac{n^2-1}{2n^2+1} \tag{13}$$

In the case under study, the solvatochromic shift of the absorption spectra is described by the following relations:

$$\text{for BODD}:\quad\bar{\nu}_A=24489-1467\,f(\varepsilon,n)\quad(r=0.94) \tag{14}$$

$$\text{for BTDB}:\quad\bar{\nu}_A=24180-1424\,f(\varepsilon,n)\quad(r=0.92) \tag{15}$$

From the above correlations, the Onsager's cavity radius and μ_g-values obtained from quantum calculations, μ^{FC} could be calculated. The obtained values are smaller than the dipole

Table 4
Slopes of solvatochromic plots (m_1 and m_2), dipole moments of the ground (μ_g) and excited states (μ^{FC} and μ_e)

Diene	m_1 (cm^{-1})	m_2 (cm^{-1})	μ_g[a] (D)	μ_g[b] (D)	μ_e[b] (D)	μ_e[c] (D)	μ^{FC} (D)
BODB	5348	8904	3.6	3.9	15.8	14.4	10.2
BTDB	7577	11081	3.8	3.6	19.0	20.2	10.5

[a] Obtained from semiempirical calculations.
[b] Calculated using Eq. (5).
[c] Calculated from the ratio method, Eq. (6).

moments of the fluorescent state μ_e (see Table 4). This fact indicates the existence of a more relaxed excited state, due to ICT favored by the co-operative effects of the dimethylaniline moiety as a donor and the benzazole group as an acceptor. The direction of the ICT is supported by the calculated charge densities on the molecular sub-units, Table 3, as well as the protonation effect, see later. The hypothetical LE and ICT fluorescence maxima in the gas phase can be obtained from the intercept of the solvatochromic shifts, though they contain some uncertainty. Then, one can estimate the energy gap between the LE and ICT states of an isolated molecule. Using the intercepts in Eqs. (7–10), the energy gaps were estimated to be about 3997 and 3753 cm^{-1} for BODB and BTDB, respectively, and increase to about 6000 cm^{-1} in polar solvents like DMF.

3.3. Viscosity effect on the fluorescence characteristics

The dienes under study are expected to be fully conjugated in the ground state (optimized geometry of the ground state shows that BODB and BTDB molecules favor the planar or flat configuration). However, following excitation, rotation around certain bonds can occur leading to formation of a non-planar or twisted ICT state (TICT). The formation of such an excited state can explain the large red shifted and the high sensitivity of fluorescence to solvent polarity. To study the role of molecular flexibility in fluorescence behaviour of BODB and BTDB and to gain better information about the nature of their emitting state, the fluorescence spectra have been studied in MeOH–glycerol mixtures as well as in glycerol at different temperatures. The basic idea is to control the local viscosity of the solvent without greatly altering the polarity of the solution. This is helpful to get information about the effect of viscosity on the dynamics and fluorescence properties as well as charge transfer process. Fig. 4 shows the fluorescence spectra of BTDB in MeOH–glycerol mixtures. It clearly shows that the intensity of the long-wavelength shoulder enhances greatly as the percentage of glycerol increases in methanol solution with red shift of the peak position. BODB shows a similar behaviour but the two peaks are merged. The red shift could be easily explained from polarity point of view, where glycerol is more polar than methanol ($\varepsilon \sim 42.5$ and 32.7 at 25 °C, respectively). The fluorescence enhancement could be explained on the basis of increased viscosity, which hinder rotational motions responsible for energy dissipation and lowering of the fluorescence yield. As seen from Table 1, the fluorescence quantum yield enhances greatly on going from non- to highly viscous solvents.

Since the intensity of both overlapped bands increases as the viscosity increases, one can conclude that the large Stokes-shifted emission cannot be attributed to population of TICT state. This is due to the fact that free rotation and formation of TICT state is not favored in viscous solvents. That is to say the fluorescence intensity of the TICT should decrease with increasing viscosity. So, we believe that the skeleton of the excited dienes is basically planar, since planarity is commonly regarded as a positive structural factor in enhancing the molecular fluorescence [47]. The absence of TICT process is further confirmed by studying the effect of temperature on the fluorescence of both dienes in glycerol. As clearly shown in Fig. 5, the fluorescence intensity of BODB decreases steadily as the temperature is increased, without any change in the shape of the band. As the temperature is increased, a point is reached where free rotation and formation of TICT state is coming into play, which is not observed here. This is consistent with the results reported for 9,9′-bianthryl in glycerol and dimethylsulfoxide [48,49].

The effect of viscosity (η) on ϕ_f has been treated according to the simple relation [50,51]:

$$\phi_f = B(\eta/T)^{\alpha} \quad (16)$$

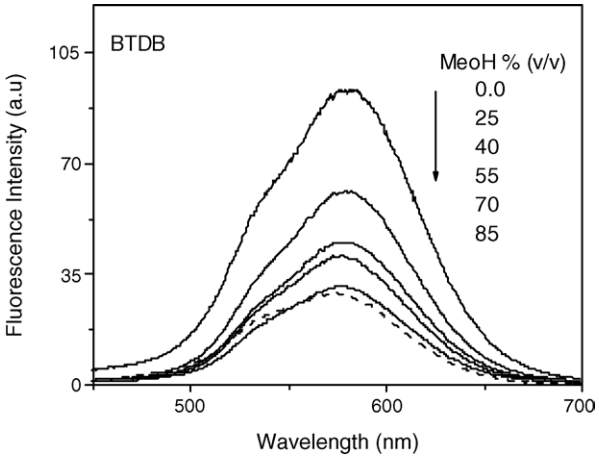

Fig. 4. Fluorescence spectra of BTDB in glycerol–methanol mixtures measured at room temperature. The ratios of methanol in glycerol (vol.%) are shown in the figure.

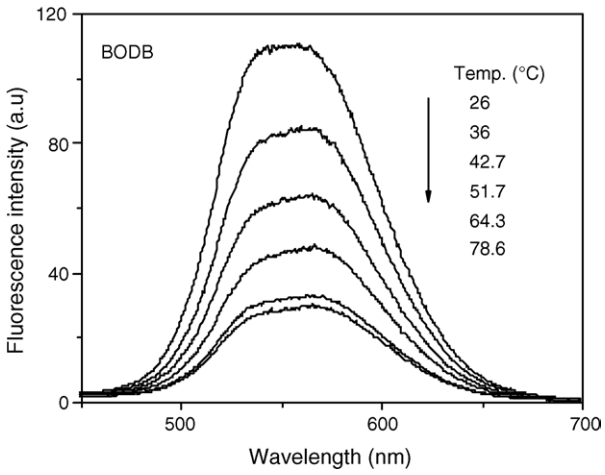

Fig. 5. Temperature dependent fluorescence spectra of BODB measured in glycerol at the indicated temperatures.

where B is a constant, T the absolute temperature and α is a fraction value reflecting the degree of sensitivity of flexible molecules to viscosity of the medium. The obtained correlations are:

$$\log \phi_f = -1.63 + 0.413 \log(\eta/T) \quad \text{for BODB} \tag{17}$$

$$\log \phi_f = -1.91 + 0.358 \log(\eta/T) \quad \text{for BTDB} \tag{18}$$

The correlation coefficients are greater than 0.99. These results suggest a free-volume dependent relaxation process competing with the fluorescence emission in highly viscous solvents [51]. Also, the values of α reflect a high degree of sensitivity of these dienes towards viscosity, thus, suggesting their valuable use as probes to explore microscopic viscosity in biologically important systems like micelles and proteins.

3.4. Prototropic equilibria and pH-dependent dual absorption and emission of BODB and BTDB

The basic absorption and emission features of BODB and BTDB in buffer solutions having different pH/H_o-values (from 6.0 to −1.0) are shown in Fig. 6. The spectral variations indicate the possibility of using of both dienes for either absorption or fluorescence-based pH sensing. As can be deduced from Fig. 6, both the long-wavelength absorption and emission bands are enhanced with increasing the pH. Also, for BTDB an ill-defined absorption band appears around 550 nm at lower pH-values. The isosbestic points at 372 and 383, 526 nm for BODB and BTDB, respectively, indicate a ground state acid–base equilibrium involving two species. The fluorescence spectra also show well-defined isoemissive points at 516 and 523 nm for BODB and BTDB, respectively. From the inflection point of the spectrophotometric titration curves (curves not shown), the ground state pK_a-values were determined and listed in Table 5 together with the spectral maxima of the different species. The fluorometric titration curves (not shown also) yield very similar pK_a-values. The appearance of dual fluorescence of the acid and base species over a large pH range (1.5–5.0) as well as the similarity of the pK_a-values obtained from spectrophotometric and fluorometric titration curves point to a slow prototropic equilibrium in the excited singlet state. This means that the radiative deactivation competes successfully with the proton dissociation process [52].

The different spectral bands, which appear in buffer solutions, can be assigned taking into consideration that the

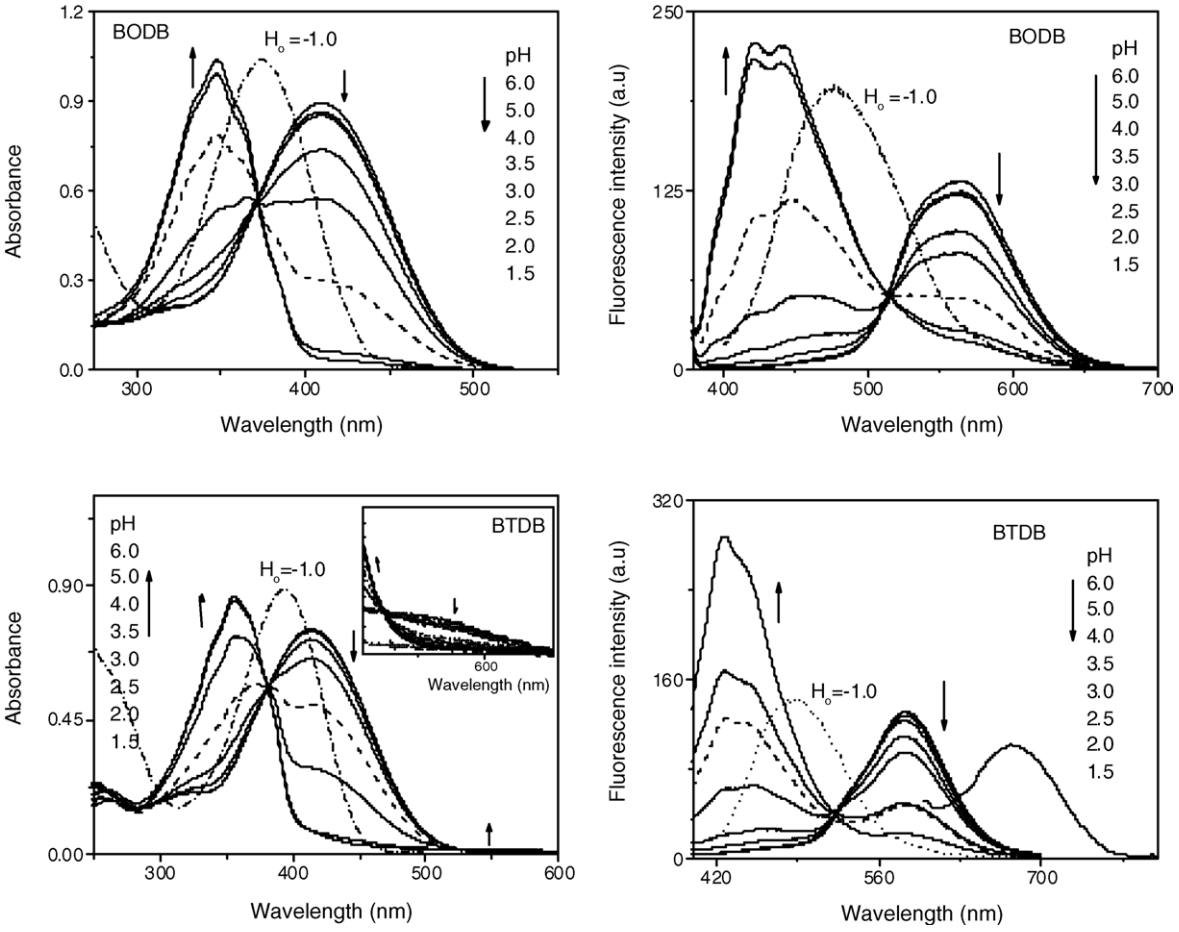

Fig. 6. pH dependent absorption and emission spectra of BODB and BTDB in 30% (v/v) ethanol–water for solubility requirements. The pH-values are indicated. The emission of BTDB around 675 nm was recorded at pH 1.5, $\lambda_{ex.}$ = 565.

Table 5
Spectral maxima of the different prototropic species as well as the ground and excited state protonation constants (pK_a- and pK_a^*-values, respectively)

Diene	Species	λ_a (nm)	λ_f (nm)	Equilibrium	pK_a	pK_a[a]	pK_a^*
BODB	Neutral	410	565	Neutral = cation I	2.88	2.93	−8.23
	Cation I	348	423	Cation I = dication	−0.054	–	4.15
	Dication	376	477				
BTDB	Neutral	415	585	Neutral = cation I	2.92	2.86	−8.01
	Cation I	357	428	Neutral = cation II	2.92	–	11.7
	Cation II	565	675	Cation I = dication	−0.26	–	5.01
	Dication	393	487	Cation II = dication	−0.26	–	−15.2

[a] From fluorometric titration.

molecules contain two basic sites (N-atoms of the amino group and the heteroring) as well as the ICT interactions. Based on the ICT interaction, it is expected that the N-atom of the heterocyclic ring would be protonated first. In fact, ground state semiemperical calculations showed that the net charges are significantly different for both N-atoms, Table 3. The maximum negative charge (−0.26) was observed at the N-atom of the dimethylamino group, which favors its protonation first. Therefore, the low energy absorption and fluorescence band is due to the ICT electronic transition in the neutral BODB and BTDB. This is confirmed by the pronounced red shift of its maximum on increasing the solvent polarity as discussed previously. On the other hand, the higher energy absorption and fluorescence band is due to dimethylamino protonated molecules (monocation I). This assignment is consistent with the complete withdrawal of the lone pair of electrons of the amino nitrogen atom from the π-electron system upon its protonation, thus, quenching the ICT interaction. This shifts the spectra to the blue side relative to the neutral counter part. Finally, the appearance of large red shifted absorption and fluorescence bands in the case of BTDB (at 565 and 675 nm, respectively) at lower pH-values, can be attributed to protonation of the N-atom of the benzothiazole ring (monocation II). Addition of a proton to the heterocyclic nitrogen atom increases the electron withdrawing ability of this part and enhances the charge transfer from the dimethylamino group.

In highly acidic solutions (from pH = 1.5 to H_o = −1.0) the short wavelength absorption and emission bands are shifted to the red while the long-wavelength bands are vanished (Fig. 7). The absorption spectra recorded within this acidity range exhibit well-defined isosbestic point at 359 and 375 nm for BODB and BTDB, respectively, indicating an acid–base equilibrium between two species (monocation I and dication). Therefore, the species responsible for this band is the dication, which is formed as a result of protonation of both nitrogen atoms.

Based on the experimental results given above, the prototropic equilibria of 1-(2-benzazolyl)-4-(*p*-dimethylaminophenyl)buta-1,3-dienes is illustrated in Scheme 2.

The excited state protonation constant (pK_a^*) has been calculated using Forster cycle [53]. The obtained values are compiled in Table 5. As can be seen extremely negative pK_a^*-values (≈−8.0) were obtained for the $-NMe_2$ group pointing to a very weak driving force for its protonation in the excited state. This is consistent with the decrease in the basicity of the nitrogen atom of the amino group upon excitation due to charge transfer to the heterocyclic ring via the butadiene bridge. This is further supported by the very large positive pK_a^*-value calculated for the neutral–monocation II equilibrium, in the case of BTDB. For dication–monocation I equilibrium, more positive pK_a^*-values were obtained indicating that the tertiary heterocyclic nitrogen becomes more basic in the excited singlet state. In contrast, for monocation

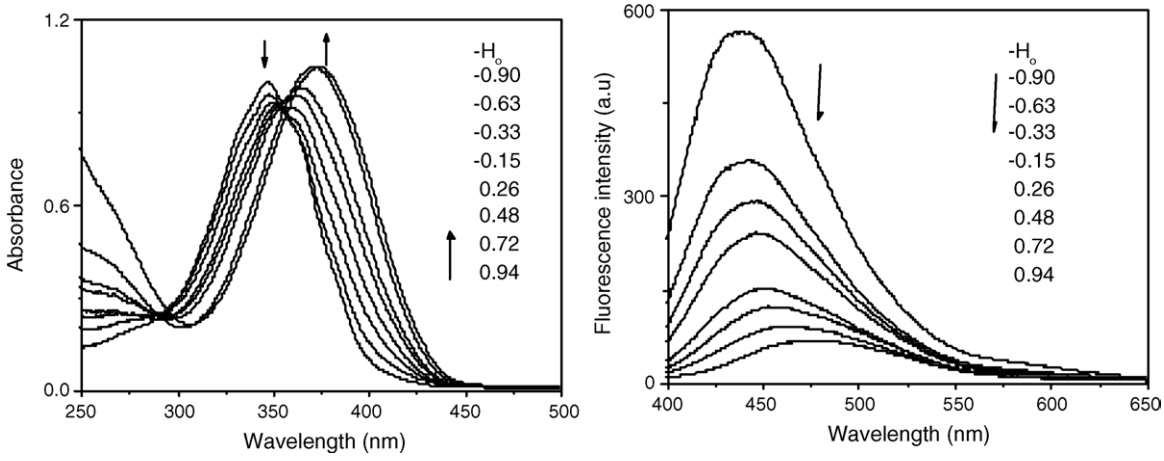

Fig. 7. Change of the absorption and fluorescence spectra of BODB recorded at lower pH/H_o-values.

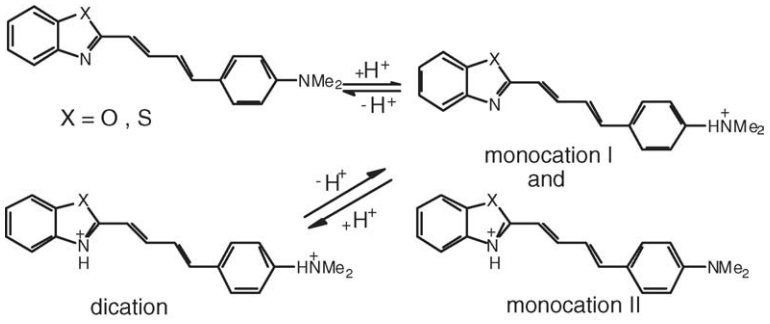

Scheme 2.

II–dication equilibrium an extremely negative pK_a^*-value was calculated indicating the drift of the electron lone pair of the amino group towards the benzazolium cation.

References

[1] W. Gartner, P. Towner, Photochem. Photobiol. 62 (1995) 1.
[2] I.M. Pepe, J. Photochem. Photobiol. B: Biol. 48 (1999) 1.
[3] A.K. Singh, M. Darshi, S. Kanvah, J. Phys. Chem. A 104 (2000) 464.
[4] D.J.S. Birch, R.E. Imhof, Chem. Phys. Lett. 88 (1982) 2.
[5] C. Rulliere, E. Declemy, Chem. Phys. Lett. 135 (1987) 213.
[6] M.T. Allen, D.G. Whitten, Chem. Rev. 89 (1989) 1691.
[7] D.G. Waldek, Chem. Rev. 91 (1991) 415.
[8] J. Oberle, L. Bramerie, G. Jonusauskas, C. Rulliere, Opt. Commun. 169 (1999) 325.
[9] M. Blanchard-Desce, V. Alain, L. Midrier, R. Wortmann, S. Lebus, C. Glania, P. Kramer, A. Fort, J. Muller, M. Barzoukas, J. Photochem. Photobiol. A: Chem. 105 (1997) 115.
[10] B.J. Coe, J.A. Harris, I. Asselberghs, K. Wostyn, K. Clays, A. Persoons, B.S. Brunschwig, S.J. Coles, T. Gelbrich, M.E. Light, M.B. Hursthouse, K. Nakatani, Adv. Funct. Mater. 13 (2003) 347.
[11] P. Plaza, D. Laage, M.M. Martin, V. Alain, M.B. Desce, W.H. Thompson, J.T. Hynes, J. Phys. Chem. A 104 (2000) 2396.
[12] C.E. Bunker, C.A. Lytle, H.W. Rollins, Y.P. Sun, J. Phys. Chem. 101 (1999) 3214.
[13] K. Sen, S. Basu, Chem. Phys. Lett. 387 (2004) 61.
[14] A.K. Singh, G.R. Mahalaxmi, Photochem. Photobiol. 71 (2000) 387.
[15] H. Braatz, S. Hecht, H. Seifert, S. helm, J. Bendig, W. Rettig, J. Photochem. Photobiol. A: Chem. 123 (1999) 99.
[16] H. El-Gezawy, W. Rettig, R. Lapouyade, Chem. Phys. Lett. (2005) 140.
[17] A.K. Singh, M. Darshi, Biochim. Biophys. Acta 1563 (2002) 35.
[18] M.T. Allen, L. Miola, B.R. Suddaby, D.G. Whitten, Tetrahedron 43 (1987) 1477.
[19] N. Di Cesare, J.R. Lakowicz, J. Photochem. Photobiol. A: Chem. 143 (2001) 39.
[20] C. Peinado, E.F. Salvador, F. Catalina, A.E. Lozano, Polymer 42 (2001) 2815.
[21] Ph. Hebert, G. Baldacchino, Th. Gustavsson, J.C. Mialocq, J. Photochem. Photobiol. A: Chem. 84 (1994) 45.
[22] G. Bartocci, G. Galiazzo, U. Mazzucato, A. Spalletti, Phys. Chem. Chem. Phys. 3 (2001) 379.
[23] G. Bartocci, G. Galiazzo, L. Lattrini, E. Marri, U. Mazzucato, A. Spalletti, Phys. Chem. Chem. Phys. 3 (2001) 379.
[24] U. Mazzucato, A. Spalletti, Photochem. Photobiol. Sci. 2 (2003) 282.
[25] I. Baraldi, A. Spalletti, D. Vanossi, Spectrochim. Acta A 59 (2003) 75.
[26] G. Bartocci, G. Galiazzo, G. Gennari, E. Marri, U. Mazzucato, A. Spalletti, Chem. Phys. 272 (2001) 213.
[27] G. Bartocci, A. Spalletti, R.S. Becker, F. Elisei, S. Floridi, U. Mazzucato, J. Am. Chem. Soc. 121 (1999) 1065.
[28] A. Spalletti, G. Bartocci, G. Galiazzo, A. Macchioni, U. Mazzucato, J. Phys. Chem. A 103 (1999) 8994.
[29] E. Marri, G. Galiazzo, U. Mazzucato, A. Spalletti, Chem. Phys. 260 (2000) 383.
[30] S.M. Bakalova, A.G. Santos, I. Timcheva, J. Kaneti, I.L. Filipova, G.M. Dobrikov, V.D. Dimitrov, J. Mol. Struct. (Theochem.) 710 (2004) 225.
[31] T.A. Fayed, J. Photochem. Photobiol. A: Chem. 121 (1999) 17.
[32] T.A. Fayed, S.S. Ali, Spect. Lett. 36 (2003) 375.
[33] T.A. Fayed, Coll. Surf. A: Physicochem. Eng. Aspects 236 (2004) 171.
[34] T.A. Fayed, S.H. Etaiw, H.M. Khatab, J. Photochem. Photobiol. A: Chem. 170 (2005) 97.
[35] M. Kawakami, K. Koya, T. Ukai, N. Tatsuta, A. Ikegawa, K. Ogawa, T. Shishido, L.B. Chen, J. Med. Chem. 41 (1998) 41.
[36] R. Garg, S.P. Gupta, Biorg. Med. Chem. 6 (1998) 1707.
[37] S. Koichi, Application, Japan Patent 87 (1987).
[38] P. Hrobarik, P. Zahradink, W.M.F. Fabian, Phys. Chem. Chem. Phys. 6 (2004) 495.
[39] C.H. Rochester, Acidity Functions, Academic Press, London, 1970.
[40] J.V. Morris, M.A. Mahaney, I.R. Huber, J. Phys. Chem. 80 (1976) 971.
[41] T.A. Fayed, G. Grampp, S. Landgraf, J. Inf. Recording 25 (2000) 367.
[42] C. Reichardt, Solvents and Solvent Effects in Organic Chemistry, 2nd ed., VCH, Weinheim, 1988.
[43] G. Krishnamoorthy, S.K. Dogra, Chem. Phys. 243 (1999) 45.
[44] E. Lippert, Ber. Bunsenges. Phys. Chem. 61 (1957) 962.
[45] A. Kawski, Z. Naturforsch 57a (2002) 255.
[46] R.M. Hermant, N.A.C. Bakker, T. Scherer, B. Krijinen, J.W. Verboeven, J. Am. Chem. Soc. 112 (1999) 1214.
[47] D. Cao, Q. Fang, D. Wang, Z. Liu, G. Xue, G. Xu, W. Yu, Eur. J. Org. Chem. (2003) 3628.
[48] F. Schneider, E. Lippert, Ber. Bunsen-Ges. Phys. Chem. 72 (1968) 1155.
[49] J. Catalan, C. Diaz, V. Lopez, P. Perez, R.M. Claramunt, J. Phys. Chem. 100 (1996) 18392.
[50] R.O. Loutfy, B.A. Arnold, Phys. Chem. 86 (1982) 4205.
[51] M.S.A. Abdel-Mottaleb, A.M.K. Sherief, A.A. Abdel-Azim, M.M. Habashy, L.F.M. Ismail, J. Photochem. Photobiol. A: Chem. 44 (1988) 161.
[52] M. Maus, K. Rurack, New J. Chem. 24 (2000) 677.
[53] T. Forster, Z. Elekrochem. 54 (1950) 531.